Isolated α-turns in peptides: a selected literature survey

Journal:	*Journal of Peptide Science*
Manuscript ID	PSC-22-0104.R1
Wiley - Manuscript type:	Review
Date Submitted by the Author:	n/a
Complete List of Authors:	Biondi, Barbara; Institute of Biomolecular Chemistry CNR, Chemical Sciences Formaggio, Fernando; University of Padova, Department of Chemistry Toniolo, Claudio; University of Padova, Peggion, Cristina; University of Padova, Crisma, Marco; Institute of Biomolecular Chemistry, CNR, Department of Chemistry, University of Padova
Keywords:	linear and cyclic peptides, X-ray diffraction, tight turns, α-turns, statistical analysis

SCHOLARONE™
Manuscripts

Isolated α-turns in peptides: a selected literature survey

Barbara Biondi[1], Fernando Formaggio[1,2], Claudio Toniolo[1,2], Cristina Peggion[1,2], Marco Crisma[1]*

[1]CNR - Institute of Biomolecular Chemistry, Padova Unit, 35131 Padova, Italy; [2]Department of Chemical Sciences, University of Padova, 35131 Padova, Italy

Correspondence

Barbara Biondi, CNR - Institute of Biomolecular Chemistry, Padova Unit, 35131 Padova, Italy
E-mail: barbara.biondi@unipd.it

KEYWORDS

statistical analysis; linear and cyclic peptides; X-ray diffraction; tight turns; α-turns

ABSTRACT

The results of classifying into various types the 68 examples of isolated α-turns in the X-ray diffraction crystal structures of *peptides* documented in the literature are presented and discussed in this review article. α-Turns characterized by the *trans* disposition of all ω torsion angles are common for the backbone linear peptides investigated. In contrast, the *cis* arrangement of the N-terminal (ω_{i+1}) torsion angle, among those generated by the three residues internal to the α-turn, is a peculiar feature of 65% of the cyclic peptides. Among linear and cyclic peptides featuring the all-*trans* disposition of the ω torsion angles, only one third of the α-turns display φ,ψ values not too far from those characterizing regular α-helices. In general, our findings, taken together, suggest that a significant conformational diversity is compatible with the formation of an intramolecularly H-bonded C_{13}-member *pseudo*cycle (α-turn) in linear and cyclic peptides.

1| INTRODUCTION

A *peptide* turn is a 3D-structural motif where the overall directionality of its main chain is reversed. The most common types of "tight" peptide turns are characterized, and in part enthalpically stabilized, by (backbone) N-H···O=C (backbone) intramolecular H-bonds. Moreover, this intramolecularly H-bonding occurrence in turns usually correlates well with space proximity (< 7Å) between the C^{α}-atoms of their terminal α-amino (carboxylic) acid constituents.

In particular, in a system of *five* linked peptide units (Figure 1) the possible conformations intramolecularly H-bonded in the traditionally called "*common way*", that is where the H-bonds go from a N-H donor *downstream* to a C=O acceptor *upstream*, are typically classified as C_7 (γ-turns), C_{10} (β-turns), C_{13} (α-turns), and C_{16} (π-turns), where C stands for *cyclo* and the subscript number indicates how many atoms are involved in the *pseudo*-annular structure closed by the intramolecular H-bond. In an alternative, accepted terminology, in a γ-turn the C^{α}-atoms of the N- and C- terminal residues of the main chain are separated by *two* (class i←i+2) peptide bonds, whereas in the β-, α- and π-turns they are separated by *three* (*i*←*i+3*), *four* (i←i+4), and *five* (i←i+5) peptide bonds, respectively.

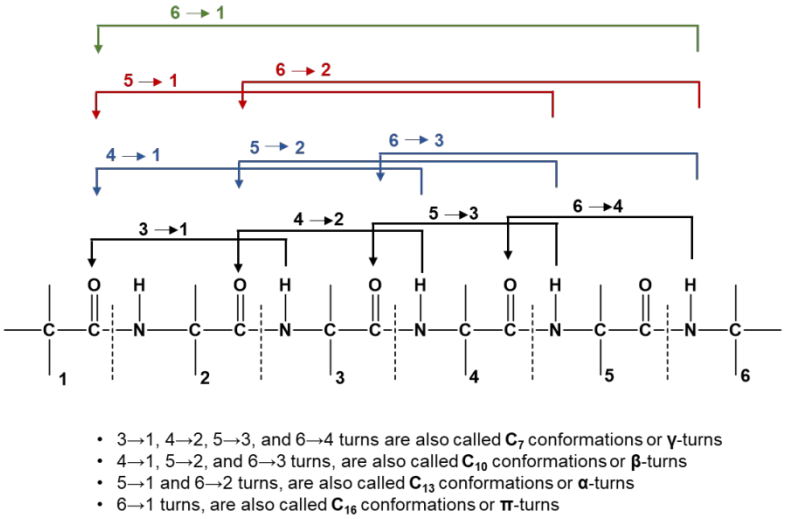

FIGURE 1. Possible backbone N-H···O=C intramolecularly H-bonded conformations in a system of five-linked peptide units. Only peptides entirely based on *α-amino (carboxylic) acids* are considered.

Review article and research papers on peptide β-turns[1-10] are extremely abundant, while those on γ-turns, although definitely less numerous,[11-21] cover this latter 3D-structural element sufficiently well. The focus of the review article discussed below is *exclusively* based on isolated peptide *α-turns* (typically, an α-turn internally encapsulates *three complete* α-amino acid residues).[22-35] A similar literature contribution on the spatially widest member of this group, the π-turn,[36-39] will be produced by the present co-authors in the near future.

To intramolecularly H-bonded, *isolated*, regular peptide α-turns, this review article will *not* add: (i) a system of two *consecutive* α-turns nor part of a system of two *concatenated* α-turns; (ii) "open" (lacking the intramolecular H-bond) α-turns; (iii) α-turns formed by *stapling*, *via* either a covalent bond or by a N-to-C terminal charge···charge interaction; (iv) α-turns in *pseudo*-peptides such as those characterized, for example, by a backbone ester bond (*depsi*-peptides) or a reduced backbone amide carbonyl; (v) α-turns based on amino acids different from α, as in the case of one δ-amino, or one β- and one γ-amino acids replacing three consecutive α-amino acids.

To avoid ambiguous conformational assignments, only definitive results from *X-ray diffraction* experiments in the *crystal* state will be taken into consideration, thereby neither including conclusions from NMR/ IR absorption/ CD physico-chemical investigations in *solution* nor those from conformational energy calculations/ predictions (algorithms)/ artificial neural networks (machine learning).

The α-turns examined here will only be those contained in short (≤ 20 amino acids) peptides, excluding those in proteins or forming a segment of the longer classical 3D-structural element *α-helix* (with three or more α-turns). Excellent substrates for this investigation are homo-chiral peptides and α-amino acid sequences with residues of mixed chirality, linear and cyclic peptides, and peptide compounds even if comprising relatively unusual 3D-structural properties, such as one (or more) *cis* backbone amide bond or embracing in the C_{13} annular conformation of the α-turn either one shorter C_7 or C_{10} intramolecularly H-bonded forms.

2| EXPERIMENTAL

A search was performed on the Cambridge Structural Database (CSD, version 5.43, including updates to March 2022)[40] for structures containing the fragment -C(=O)-[N-C-C(=O)]$_3$-NH- in which the NH_{i+4} and C_i=O_i groups are involved in a C_{13} structure, on the basis of the intramolecular H-bonding criteria that the O_i···H_{i+4} distance must be within 2.50 Å (*i.e.*, less than the sum of van der Waals radii of H and O) and the N_{i+4}-H_{i+4}···O_i angle ≥ 120°.[41-43] To this aim, the ConQuest[44] software package was exploited, which *inter alia* allowed retrieval of the values of relevant backbone torsion angles. The search returned a *total* of 309 entries (X-ray diffraction structures). As expected, most of the entries correspond either to α-helices, characterized by the occurrence of multiple, consecutive C_{13} structures, or to mixed α-/3$_{10}$-helices in which the C_{13} and C_{10} structures are variously combined. To ensure that isolated α-turns occurring in two crystallographically-independent molecules in the same entry would not escape the search, entries corresponding to linear peptides with two or less C_{13} structures, as well as entries corresponding to cyclic peptides with four or less C_{13} structures, were individually analyzed with the aid of the

program Mercury.[45] Only peptides of the two sub-groups possessing isolated C_{13} structures were retained. As for cyclic peptides, we took into consideration only molecules in which the cycle is entirely constituted of α-amino acids. In other words, molecules in which the cyclic skeleton either combines peptide and non-peptide portions, or it results from covalent bonding between two side chains (as well as from side-chain to backbone cyclization) of an otherwise linear peptide backbone were not retained.

The search described above cannot identify C_{13} structures in entries for which the coordinates of H-atoms were not deposited in the CSD, as it quite often happened in less recent years. Therefore, a second search was performed for the fragment -C(=O)-[N-C-C(=O)]$_3$-N- with the $O_i \cdots N_{i+4}$ distance less than 3.30 Å as the search criterion, returning 396 entries. This second set of entries obviously contains also the 309 entries which resulted from the first search. After removal of these latter, the remaining 87 entries were individually analyzed as above. For those entries potentially possessing isolated C_{13} structures, a check was made against the intramolecular H-bonding schemes as reported in the original publications. Only seven additional structures, all of them belonging to the class of cyclopeptides, were recovered in this way.

Overall, our survey returned 17 examples of isolated α-turns in 15 X-ray diffraction structures of linear peptides, and 51 examples of isolated α-turns in the X-ray diffraction structures of 41 cyclic peptides.

3| RESULTS AND DISCUSSION

The results of our survey on the occurrence of isolated α-turns in the X-ray diffraction structures of peptides deposited in the CSD are summarized in Table 1 (with Figure 2) and in Table 2, respectively, for linear and cyclic peptides. For each entry, the values of backbone torsion angles internal to the 13-membered H-bonded *pseudo*cycle are reported, accompanied by the available intramolecular H-bond parameters.

TABLE 1. Relevant backbone torsion angles (°) and intramolecular H-bond parameters (Å, °) for *isolated* α-turns in *linear* peptides. The amino acid sequence within each α-turn is underlined

Entry	ω_i	ϕ_{i+1}	ψ_{i+1}	ω_{i+1}	ϕ_{i+2}	ψ_{i+2}	ω_{i+2}	ϕ_{i+3}	ψ_{i+3}	ω_{i+3}	$N_{i+4}...O_i$	$H_{i+4}...O_i$	N_{i+4}-H_{i+4} ...O_i	Notes	CSD refcode	References
1	HCO-Adm-Adm-Adm-NH*i*Pr (three structures from different crystallization conditions)															46
1A	n.a.	-52	-49	-170	-59	-47	-177	-60	-60	-172	3.095	2.22	178		GOHRUT	
1B	n.a.	-53	-49	-170	-60	-46	-177	-60	-60	-173	3.096	2.22	177		GOHRUT01	
1C	n.a.	-53	-49	-170	-60	-46	-177	-60	-60	-173	3.094	2.22	177		GOHRUT02	
2	Z-Aib-Gly-L-Ile-L-Leu-OMe														LEKJOA	47
	-173	-66	-21	179	-89	-7	-177	-115	-54	176	2.958	2.15	171	(a)		
3	H-L-Tyr-D-Tic-L-Phe-L-Phe-NH_2 (two independent molecules, A and B)														CALFEB	48
3A	167	62	-146	-168	-58	-49	-163	-129	3	n.a.	3.086	2.34	145			
3B	177	65	-160	-167	-88	-16	-179	-109	-18	n.a.	3.194	2.49	139	(b)		
4	Piv-D-Pro-L-Pro-D-Ala-NHMe														LOCSUS	49
	-173	61	-154	180	-86	31	169	129	34	175	2.849	2.02	162	(a)		
5	L-pGlu-L-Asn-L-Pro-D-Tyr-D-Trp-NH_2														NOPZUO	50
	167	-59	153	178	71	39	167	93	24	n.a.	2.965	2.17	150			
6	Ac-MeDeg-Deg-Deg-Deg-$N(Et)_2$													(a,c)	POQRIX	51
	-173	-49	-53	-171	-57	-40	-172	-66	-43	-170	3.196	2.40	154			
7	Boc-L-Val-Aib-D-Ala-L-Leu-NHMe														ICUWUA	52
	176	59	19	-176	81	1	-171	-112	-36	-178	3.055	2.22	163	(a,d)		
8	(complex imido)-L-Ala-L-Ala-L-Ala-NHPh													(a,c)	ADOZOI	53
	-164	-60	-47	-178	-63	-40	-171	-82	-30	-173	2.962	2.15	151			
9	Ac-Gly-L-Ala-L-Ala-L-Ala-NH_2 (two independent molecules, A and B, each encapsulated by a synthetic host)														CUDYIK	54
9A	177	-49	-50	-177	-77	-24	171	-68	-22	-178	2.812	2.13	134	(e)		
9B	175	-47	-38	-178	-84	-42	179	-53	-31	-172	2.980	2.26	139	(e)		

10	Boc-L-Ile-Aib-L-Leu-L-Phe-L-Ala-OMe (two independent molecules, A and B)													(a, c, f)	FASRAU	55
10B	177	-49	-38	-174	-71	-21	-173	-115	-7	-174	2.979	2.42	123			
11	Piv-L-Pro-Ac_3c-L-Val-NHMe													(g)	HOHLEW	56
	-178	-66	143	-177	74	2	-176	-130	-50	-176	2.852	1.86	150			
12	Z-Aib-Aib-L-Glu(OMe)-L-Ala-L-Lol													(a, h)	IRIDOC	57
	-173	-58	-26	180	-75	-24	-172	-109	-25	-175	3.085	2.31	150			
13	Boc-L-δOPhe-L-Val-Aib-L-Leu-NH*i*Pr													(a, i)	TIVYOP	58
	-179	-57	-35	-178	-62	-27	-174	-94	-32	-172	3.101	2.36	144			

n.a.: Data not available. Chemical structures for the non-coded α-amino acids are provided in Figure 2.

(a) C_{10} structure (N_{i+3}-H...O_i) within the C_{13} structure. (b) Water-mediated C_{10} structure (N_{i+3}-H...OH_2...O_i) within the C_{13} structure. (c) Only one of the two independent molecules. (d) A non-helical C_{10} structure (type-II' β-turn) with L-Val and Aib as corner residues precedes the C_{13} structure. (e) The C_{13} structure is followed by a helical C_{10} structure (type-III β-turn) with L-Ala(3) and L-Ala(4) as corner residues. (f) A helical C_{10} structure (type-III β-turn) with L-Ile(1) and Aib(2) as corner residues precedes the C_{13} structure. (g) A non-helical C_{10} structure (type-II β-turn) with L-Pro and Ac_3c as corner residues within the C_{13} structure. (h) A helical C_{10} structure (type-III β-turn) with Aib(1) and Aib(2) as corner residues precedes the C_{13} structure. (i) A helical C_{10} structure (type-III β-turn) with L-δOPhe(1) and L-Val(2) as corner residues precedes the C_{13} structure.

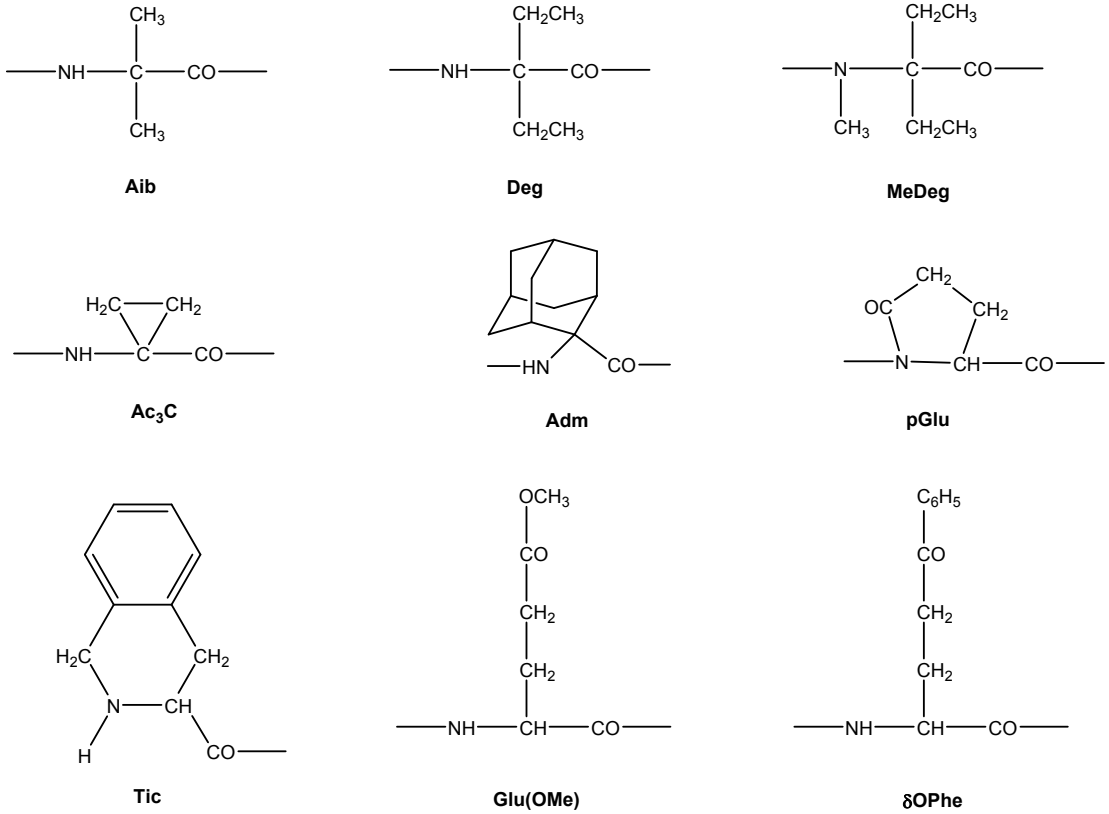

FIGURE 2. Chemical structures for the non-coded α-amino acids mentioned in Table 1.

TABLE 2. Relevant backbone torsion angles (°) and intramolecular H-bond parameters (Å, °) for *isolated* α-turns in *cyclic* peptides. The amino acid sequence within each α-turn is underlined. Starred residues indicate side-chain modification(s)

Entry	ω_i	ϕ_{i+1}	ψ_{i+1}	ω_{i+1}	ϕ_{i+2}	ψ_{i+2}	ω_{i+2}	ϕ_{i+3}	ψ_{i+3}	ω_{i+3}	$N_{i+4}...O_i$	$H_{i+4}...O_i$	N_{i+4}-H_{i+4} ...O_i	Notes	CSD refcode	References
Pentapeptides																
1	c-[Aib-L-Phe-Gly-D-(αMe)Phe-L-Pro]													(a)	FUBYAE	59
	-177	-51	-45	-177	-86	54	-174	52	35	-178	2.980	2.25	162			
2	c-(Gly-L-Pro-D-Phe-L-Ala-L-Pro) trihydrate														GICHOP	60
	-172	64	-143	-176	-68	-45	177	-74	-31	-176	2.916	2.33	139			
Hexapeptides																
3	c-(L-Ala-D-Ala-L-MeTyr-L-Ala-L-MeTyr*-L-MeTyr*) chloroform ethanol solvate hemihydrate													(b)	OHUXAQ	61
	172	-117	102	5	-89	164	164	140	-42	-179	3.098	2.15	173			
Heptapeptides																
4	Ilamycin B1; c-(L-Ala-L-MeLeu-L-Leu-L-Nva-L-Trp*-L-Leu-L-Tyr*) ethanol solvate monohydrate													(c)	ILAMYC	62
	-175	-61	126	-11	-121	38	-168	-123	2	165	3.320	n.a.	n.a.	(d)		
5	Ilamycin B_2; c-(L-Ala-L-MeLeu-L-Leu-L-Nle*-L-Trp*-L-MeLeu-L-Tyr*)														VEHFOG	63
	-169	-68	146	-17	-106	57	-178	-106	-46	-174	3.208	2.37	165	(d)		
6	Ilamycin D; c-(L-Ala-L-MeGlu*-L-Leu-L-Nle*-L-Trp*-L-MeLeu-L-Tyr*)														VEHGAT	63
	-172	-71	147	-12	-105	57	180	-107	-48	-164	3.266	2.44	156	(d)		
7	Ilamycin F; c-(L-Ala-L-MeGlu*-L-Leu-L-Nle*-L-Trp*-L-MeLeu-L-Tyr*)													(a)	VEHGEX	63
	-169	-67	143	-17	-107	53	-179	-99	-46	-172	3.292	2.47	162	(d)		
8	Ilamycin H; c-(L-Ala-L-MeGlu*-L-Leu-L-Nle*-L-Trp*-L-MeLeu-L-Tyr*)														RUSPUT	64
	-173	-64	139	0	-111	37	-176	-102	-38	-169	3.282	2.45	159	(d)		
9	Axinellasin A; c[L-Asn-L-Pro-L-Met(SO)-L-Leu-L-Leu-L-Pro-L-Val] (*S* configuration at sulfoxide)														MAVFAU	65
	180	-63	147	8	-98	10	-172	-95	-22	-171	3.163	2.44	140	(d)		
10	Axinellasin B; c[L-Asn-L-Pro-L-Met(SO)-L-Leu-L-Leu-L-Pro-L-Val] (*R* configuration at sulfoxide)														MAVFEY	65

	180	-64	145	10	-97	10	-174	-97	-18	-168	3.031	2.38	131	(d)	
11	Axinellasin C; c[L-Asn-L-Tyr-L-Phe-L-Phe-L-Pro-L-Pro-L-Met(SO)] (*S* configuration at sulfoxide)													(a)	MAVFIC	65
	-176	-68	152	7	-93	15	174	-81	-34	176	3.268	2.43	159			
12	Cordyheptapeptide A; c-(D-MePhe-L-Pro-Sar-L-Phe-L-MeTyr-L-Ile-L-Leu) hydrate													(c)	XEDKOH	66
	-163	124	-74	-7	-77	174	175	107	-12	178	2.835	1.97	165			
13	Cordyheptapeptide C; c-(Sar-L-Phe-D-MeTyr-L-Val-L-Leu-D-MePhe-L-Pro) methanol solvate monohydrate														BEMVAS	67
	164	124	-78	16	-84	172	171	108	-11	174	2.914	2.11	172			
14	Euryjanicin A; c-(L-Trp-L-Pro-L-Ile-L-Ser-L-Phe-L-Val-L-Pro)														NUCZUH	68
	178	-65	139	6	-100	6	-179	-58	-46	174	3.289	2.43	174	(d)		
15	Isophakellistatin 3; c-(Gly-L-Pro-L-Thr-L-Leu-L-Pro*-L-Pro-L-Phe) acetone solvate monohydrate														SUMNOD	69
	173	-53	138	10	-95	9	-173	-89	-35	-173	3.176	2.34	156	(d)		
16	Evolidine; c-(L-Ser-L-Phe-L-Leu-L-Pro-L-Val-L-Asn-L-Leu) tetrahydrate														TALVAD	70
	-175	-65	151	2	-93	13	-176	-95	-16	-172	3.082	2.09	178	(d)		
17	Pseudostellarin D; c-(Gly-L-Tyr-Gly-L-Pro-L-Leu-L-Ile-L-Leu) acetonitrile solvate monohydrate														ZORRED	71
	-173	-56	126	180	89	-15	-172	-113	-53	180	3.027	2.02	150			
Octapeptides																
18	[(*S*)-Sulfoxide]-6'-O-methyl-α-amanitin; bicyclo-(L-Asn-L-Hyp-L-Ile*-L-Trp*-Gly-L-Ile-Gly-L-Cys*)													(e)	CAZFIS10	72
	-175	-61	-31	177	-66	-42	-171	-81	-52	-178	2.998	2.30	148			
19	6'-O-Methyl-S-oxo- α -amanitin-sulfone; bicyclo-(L-Asn-L-Hyp-L-Ile*-L-Trp*-Gly-L-Ile-Gly-L-Cys*)													(e)	CAZFOY10	72
	-174	-62	-31	178	-67	-42	-172	-81	-47	-179	2.996	2.30	124			
20	β-Amanitin; bicyclo-(L-Trp*-Gly-L-Ile-Gly-L-Cys*-L-Asp-L-Hyp-L-Ile*)													(e)	BAMANT10	73
20a	-175	-59	127	-176	88	-4	-173	-121	-85	179	3.163	2.44	128	(d,f)		
20b	-174	-61	-37	-172	-79	-23	-169	-109	-40	173	2.926	1.95	161	(d,g)		
21	S-Deoxo(Ile^3)amaninamide; bicyclo-(L-Asn-L-Hyp-L-Ile-L-Trp*-Gly-L-Ile-Gly-L-Cys*)													(e)	COBLUA	74
21a	180	-48	131	179	83	1	-166	-134	-76	178	3.150	2.25	157	(d,f)		
21b	-174	-68	-17	-179	-99	-48	180	-77	-27	166	2.908	2.16	143	(h)		
22	S-Deoxo-(γ(*R*)-hydroxy- Ile ^{3})amaninamide; bicyclo-(L-Asn-L-Hyp-L-Ile*-L-Trp*-Gly-L-Ile-Gly-L-Cys*)													(e)	JAWTIK	75

22a	-172	-73	-14	178	-98	-35	-176	-93	-24	165	2.863	n.a.	n.a.	(g)		
22b	-175	-52	136	-179	80	0	-167	-132	-88	-178	3.184	n.a.	n.a.	(d,f)		
23	Bicyclo-(L-Cys-Gly-L-Pro-L-Phe-L-Cys-Gly-L-Pro-L-Phe) tetrahydrate														DUVGOQ10	76
	-168	-63	-23	-179	-96	1	-163	-126	-60	-174	3.108	2.40	126	(d,i)		
24	c-(L-Ala-Gly-L-Pro-L-Phe-L-Ala-Gly-L-Pro-L-Phe) tetrahydrate														JINGAO	77
	-168	-64	-20	-178	-97	-6	-169	-123	-54	-175	3.170	2.48	150	(d)		
25	Ribifolin racemate; c-(Gly-Ser-Ile-Ile-Leu-Gly-Ile-Leu) dihydrate													(j)	RIWZOP	78
	176	-63	-38	178	-67	-46	-175	-80	-27	-172	2.860	2.11	145			
26	c-(D-Leu-L-Asp-D-Leu-L-Orn-D-Leu-L-Asp-D-Leu-L-Orn-)														VAJPUV	79
26a	173	65	-135	176	-94	20	167	123	59	-179	2.902	2.07	157	(d)		
26b	175	62	-140	178	-97	27	158	125	60	-166	2.882	2.10	148	(d)		
Nonapeptides																
27	Cyclolinopeptide A c-(L-Pro-L-Pro-L-Phe-L-Phe-L-Leu-L-Ile-L-Ile-L-Leu-L-Val)														n.a.	80
	177	-64	161	9	-91	-16	-176	-99	-47	-170	3.34	n.a.	n.a.			
28	Cyclolinopeptide A; c-(L-Pro-L-Pro-L-Phe-L-Phe-L-Leu-L-Ile-L-Ile-L-Leu-L-Val) 2-propanol solvate monohydrate														GIPKAR10	81
	176	-60	160	10	-90	-18	-176	-97	-49	180	3.06	n.a.	n.a.			
29	Cyclolinopeptide A c-(L-Pro-L-Pro-L-Phe-L-Phe-L-Leu-L-Ile-L-Ile-L-Leu-L-Val) acetonitrile solvate														UBADEJ	82
	-169	-88	158	4	-93	-7	-168	-98	-20	-176	2.834	2.08	144			
30	Cyclolinopeptide A analog c-(L-Pro-L-Pro-L-Phe-L-Phe-Aib-Aib-L-Ile-D-Ala-L-Val) methanol solvate dihydrate														JUJHUR	83
	175	-66	163	9	-90	-17	-176	-97	-43	-171	3.063	n.a.	n.a.			
31	Cyclolinopeptide B; c-(L-Ile-L-Pro-L-Pro-L-Phe-L-Phe-L-Val-L-Ile-L-Met-L-Leu) methanol solvate														SAFVOM	84
	-174	-77	157	-10	-91	-5	-167	-99	-24	-171	2.957	2.18	153			
32	Cyclolinopeptide K; c-[L-Met(SO_2)-L-Leu-L-Ile-L-Pro-L-Pro-L-Phe-L-Phe-L-Val-L-Ile] butanol solvate monohydrate														AYUQIV	85
	-179	-77	163	2	-90	-4	-169	-94	-21	174	2.862	2.14	144			
33	c-(L-Val-L-Leu-L-Pro-L-Ile-L-Leu-L-Leu-L-Leu-L-Leu-L-Val-L-Leu-) monohydrate														LETPIM	86
	-178	-80	157	-5	-94	-7	-175	-118	-24	-170	2.965	2.39	123			
34	c-(L-Pro-L-Pro-L-Phe-L-Phe-Aib- Aib-L-Ile-D-Ala-L-Val) acetonitrile solvate dihydrate														LINCOA	87

	176	-67	162	8	-90	-16	-175	-97	-40	-171	2.999	2.28	132		
Decapeptides															
35	Antamanide; c-(L-Val-L-Pro-L-Pro-L-Ala-L-Phe-L-Phe-L-Pro-L-Pro-L-Phe-L-Phe) octahydrate acetonitrile solvate													ANTAHC10	88
35a	176	-64	161	3	-80	-20	-165	-103	-22	172	2.853	n.a.	n.a.	(k)	
35b	168	-62	160	4	-92	-4	-177	-101	-22	174	2.883	n.a.	n.a.	(l)	
36	(Phe^4,Val^6)-Antamanide; c-(L-Val-L-Pro-L-Pro-L-Phe-L-Phe-L-Val-L-Pro-L-Pro-L-Phe-L-Phe) trihydrate													PVANTS	89
36a	177	-67	153	5	-98	4	-170	-97	-35	177	2.896	n.a.	n.a.	(k)	
36b	177	-67	153	5	-98	4	-170	-97	-35	177	2.896	n.a.	n.a.	(l)	
37	(Phe^4,Val^6)-Antamanide; c-(L-Val-L-Pro-L-Pro-L-Phe-L-Phe-L-Val-L-Pro-L-Pro-L-Phe-L-Phe) dodecahydrate													PAANTD01	90, 91
37a	173	-65	156	6	-96	3	-170	-110	-26	171	2.884	2.02	154	(k)	
37b	173	-65	156	6	-96	3	-170	-110	-26	171	2.884	2.02	154	(l)	
38	(Thiaprolyl)^7-antamanide c-(L-Val-L-Pro-L-Pro-L-Phe-L-Phe-L-Val-L-Pro*-L-Pro-L-Phe-L-Phe) octahydrate													VEDJOD	92
38a	-178	-64	158	-3	-79	-20	-169	-98	-22	176	2.830	2.01	138	(k)	
38b	165	-64	161	2	-95	-1	-176	-94	-27	-179	2.986	2.08	149	(l)	
39	c-(L-Phe-L-Pro-L-Pro-L-Ala-L-Phe-L-Phe-L-Pro-L-Pro-L-Ala-L-Phe) tetrahydrate													HEBKUU	93
39a	173	-70	165	-1	-88	-4	-178	-92	-26	175	2.797	2.00	137	(k)	
39b	176	-72	160	1	-93	-3	-177	-89	-28	180	2.886	2.26	142	(l)	
40	Phakellistatin 8; c-(L-Pro-L-Pro-L-Ile-L-Phe-L-Val-L-Leu-L-Pro-L-Pro-L-Tyr-L-Ile) methanol solvate hydrate													NEHYAA01	94
	167	-65	152	7	-90	2	-173	-88	-45	174	2.905	2.07	164		
Dodecapeptides															
41	c-(L-Ala-L-Pro-Gly-L-Val-Gly-L-Val-L-Ala-L-Pro-Gly-L-Val-Gly-L-Val) trihydrate													FILPEW	95
41a	-178	-61	134	180	81	-3	-179	-122	-53	-173	3.020	2.12	180	(d,k)	
41b	167	-56	132	-179	70	18	177	-131	-59	-162	2.980	2.08	172	(m)	

n.a.: Data not available.

(a) Only one of the two independent molecules. (b) Ether bridge beween MeTyr*(5) and MeTyr*(6).

(c) Sign of torsion angles and configuration of amino acids as reported in the original publication. Conversely, the coordinates deposited in the CSD correspond to the other enantiomorph, for which each torsion angle has opposite sign.

(d) C_{10} structure within the C_{13} structure.
(e) Bridge between side chains of Trp* and Cys*. (f) Sequence L-Ile-Gly-L-Cys*. (g) Sequence L-Hyp-L-Ile*-L-Trp*. (h) Sequence L-Hyp-L-Ile-L-Trp*.
(i) Disulfide bridge between the two Cys residues.
(j) Structure of the racemate. The reported torsion angles refer to the all-L enantiomer.
(k) Sequence 2-3-4. (l) Sequence 7-8-9. (m) Sequence 8-9-10.

3.1| α-Turn classification

The overall distribution of the ϕ,ψ sets of residues occupying positions i+1, i+2, and i+3 internal to each α-turn for both linear and cyclic peptides is illustrated in Figure 3. To classify the conformation of each residue, we followed an approach similar to that exploited by Dasgupta *et al*.[25] in their analysis on the occurrence of α-turns (identified on the basis of a $C^{\alpha}\cdots C^{\alpha}$ distance criterion) in high resolution X-ray diffraction structures of proteins. Cluster analysis in their very large dataset led to the partitioning of the left half of the Ramachandran map (characterized by negative ϕ values) in the following main areas: "A" (right-handed helical) the entire region $-180° \leq \phi \leq -15°$, $-90° \leq \psi \leq 40°$; "E" (extended) the region characterized by negative ϕ values and $90° \leq \psi \leq 180°$; "D" the region bridging the two above. The "E" region was further divided, depending on whether the ϕ values are closer to those typical of type-II poly(Pro)$_n$ (–75°) or β-strand (–135°) conformation.

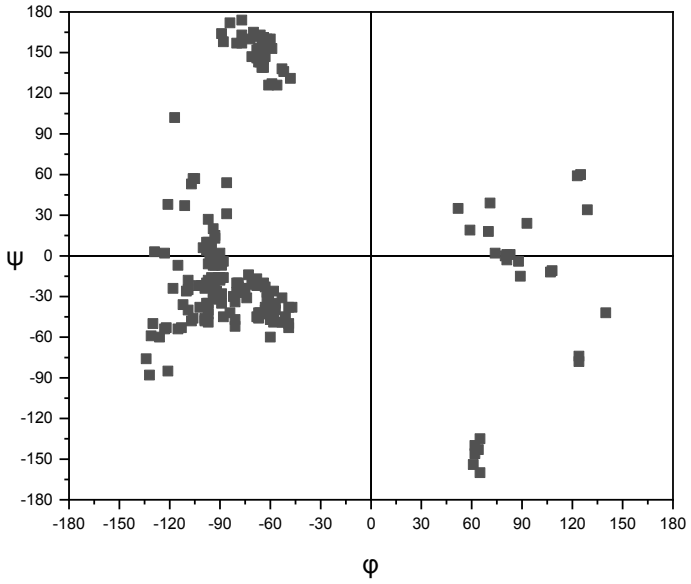

FIGURE 3. Distribution of ϕ,ψ torsion angles for residues at positions i+1, i+2, and i+3 internal to isolated α-turns in the X-ray diffraction structures of peptides.

In our opinion, labeling as right-handed helical a residue characterized by any negative value of ϕ and a *positive* value of ψ up to 40° could be confusing. Also, it would be appropriate to discriminate between ϕ,ψ values reasonably close to those typical of regular α-helices from those

possessing larger deviations. Therefore, we describe the conformation of each residue in our dataset as belonging to one of the following areas of the Ramachandran map:

- "H1" (right-handed helical), $-105° \le \phi \le -30°$, $-65° \le \psi \le -15°$;
- "H2" (distorted right-handed helical), $-150° \le \phi \le -105°$, $-90° \le \psi \le -15°$;
- "P" (type-II polyPro like, ϕ negative), $-130° \le \phi \le -30°$, $120° \le \psi \le 180°$;
- "B" (bridge, ϕ negative), $-150° \le \phi \le -30°$, $-15° \le \psi \le 60°$;
- "h1" (left-handed helical), $30° \le \phi \le 105°$, $15° \le \psi \le 65°$;
- "h2" (distorted left-handed helical), $105° \le \phi \le 150°$, $15° \le \psi \le 90°$;
- "p" (type-II polyPro like, ϕ positive), $30° \le \phi \le 130°$, $-180° \le \psi \le -120°$;
- "b" (bridge, ϕ positive), $30° \le \phi \le 150°$, $-60° \le \psi \le 15°$;
- "U" (undefined), none of the above, ϕ negative;
- "u" (undefined), none of the above, ϕ positive.

Then, the combination of the labels assigned to residues i+1, i+2, and i+3 provides a conformational descriptor for each α-turn in our dataset. In the following, linear and cyclic peptides will be analyzed separately.

3.2| Isolated α-turns in linear peptides

Linear peptides featuring a single α-turn range in length from N^{α}-acylated tripeptide amide (Table 1, entries 1A-1C, 4, 8, 11), *i.e.* the minimal main-chain length for the occurrence of such intramolecularly H-bonded conformation, to pentapeptide (entries 5, 10B).

Peptides 1 and 6 are composed exclusively of achiral residues. In their centrosymmetric crystals, molecules of both handedness simultaneously occur. For these entries, the deposited coordinates correspond to the enantiomorph of right-handed screw sense, taken as the asymmetric unit. Entry 8 features an all-L sequence. The sequences of the remaining entries combine L-residues with achiral (Gly, Aib, Ac_3c) and/or D-residues. Among the three residues occupying positions i+1 to i+3 internal to each α-turn, 23 are of L configuration, 7 D, and 21 achiral. Their ϕ,ψ sets are plotted in Figure 4. It can be seen that all of the L residues are characterized by negative values of ϕ, while the opposite holds true for the D residues. The overwhelming majority of achiral residues (19 out of 21 occurrences) join the L-residues in the left half of the Ramachandran map. The two exceptions, featuring positive ϕ values, are an Aib residue in the sequence Aib-D-Ala-L-Leu (entry 7), and an Ac_3c residue in the sequence L-Pro-Ac_3c-L-Val (entry 11).

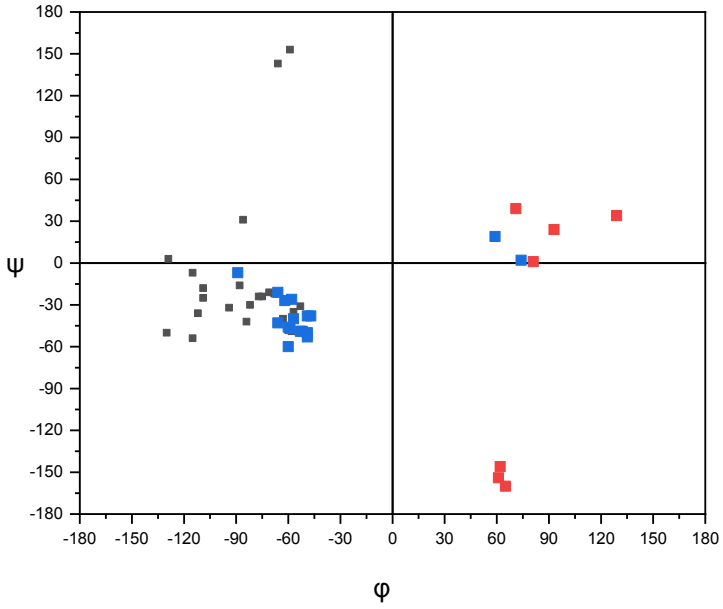

FIGURE 4. Distribution of ϕ,ψ torsion angles for residues at positions i+1, i+2, and i+3 internal to isolated α-turns in the X-ray diffraction structures of linear peptides. Residues of L configuration in black, D in red, achiral in blue.

All of the ω torsion angles in these linear peptides are found in the usual *trans* disposition, even for tertiary amide / peptide bond involving a Pro or an N^{α}-methylated residue (entries 4-6, 11). In general, deviations from the exact *trans*-planarity (180°) do not exceed ±10°. Slightly larger deviations, in the range 12° - 17° are found for ω_i, ω_{i+1} and ω_{i+2} of entry 3A, ω_{i+1} of entry 3B, and ω_i of entry 8 (Table1).

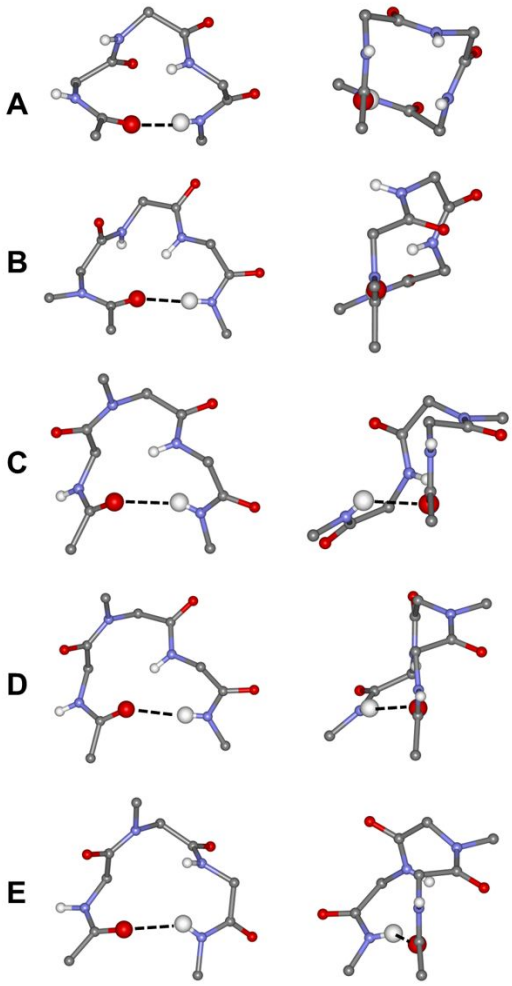

FIGURE 5. Front view (left) and side view (right) models of the five most populated types of isolated α-turns. (A) H1H1H1, (B) PbH2, (C) P*cis*BH1, (D) P*cis*BH2, (E) P*cis*H1H1.

In nearly one half of the α-turns in Table 1 (8 examples out of 17) the residues i+1, i+2, and i+3 belong to the "H1" (right-handed helical) region of the ϕ,ψ space according to our classification. Therefore, the α-turn adopted by entries 1A-1C, 6, 8, 9A-9B, and 13 can be defined as type H1H1H1 (model A in Figure 5). Within this group of entries, the ϕ,ψ sets for residues at position i+1 are quite narrowly distributed. Specifically, the ϕ_{i+1} values range from –60° to –47°, and the ψ_{i+1} values from –53° to –35°. The spread of values increases at position i+2 (ϕ_{i+2} from –84° to –57°, ψ_{i+2} from –47° to –24°), and even more at position i+3 (ϕ_{i+3} from –94° to –53°; ψ_{i+3} from –50° to –22°). It is worth pointing out that entries which show a closer approach of the ϕ,ψ torsion angles of all three residues (internal to the α-turn) to the α-helix canonical values (–63°,–42°), as determined by a statistical analysis of α-helices in crystalline peptides,[22,96] are entries 1A-1C, based on the Adm-Adm-Adm sequence, and entry 6 (sequence MeDeg-Deg-Deg). Both sequences are exclusively composed of C^{α}-tetrasubstituted residues.

There are two additional entries in which residues i+1 and i+2 are both right-handed helical, while residue i+3 either is distorted right-handed helical (entry 12: ϕ_{i+3},ψ_{i+3} = –109°,–25°) or it belongs to the bridge region (entry 10B: ϕ_{i+3},ψ_{i+3} = –115°,–7°). These two α-turns are termed type H1H1H2 and type H1H1B, respectively.

α-Turns of type H1H1H1, H1H1H2 and H1H1B share the possibility of the occurrence of a type-III β-turn encompassed within the α-turn (with the O_i carbonyl oxygen acting as a double acceptor of H-bond, from both the N_{i+3}-H_{i+3} and N_{i+4}-H_{i+4} groups), provided that the ϕ,ψ values of both residues i+1 and i+2 in the H1 region are sufficiently close to the standard for such a folded conformation ($\phi_{i+1},\psi_{i+1} = \phi_{i+2},\psi_{i+2}$ = –60°,–30°). This is indeed the case of entries 6, 8, 10B, 12, and 13, whereas for entries 1A-1C the β-turn H_{i+3} ... O_i separation is only slightly above the 2.50 Å limit commonly accepted for the occurrence of a C=O...H-N hydrogen bond.

Similarly, conformational descriptors of α-turns in which residue i+1 is located in the "H1" region and residue i+2 in the "B" region of the conformational space bear the potential for the occurrence of a type-I β-turn (ideal values: ϕ_{i+1},ψ_{i+1} = –60°,–30°; ϕ_{i+2},ψ_{i+2} = –90°,0°) encompassed within the α-turn. One example of this kind, among the linear peptides listed in Table 1, is provided by entry 2, for which the α-turn is classified as type H1BH2.

For all the entries in Table 1 described above (characterized by sequences composed by residues either of L configuration, or achiral, or a combination of the two thereof), residue i+1 is located in the "H1" region of the ϕ,ψ map. Conversely, there are two examples in which residue i+1 is found in the "P" (type-II polyPro like, ϕ negative) region, namely entries 5 and 11, both characterized by the occurrence of an L-Pro residue at position i+1. The sequence of entry 5, L-Pro-D-Tyr-D-Trp, is heterochiral. As the two D-residues are found in a left-handed helical conformation, we classify the α-turn of entry 5 as type Ph1h1. On the other hand, in the sequence of entry 11, L-Pro-Ac_3c-L-Val, an achiral residue at position i+2 is flanked by two L-residues. The Ac_3c residue adopts a bridge conformation characterized by a positive sign of ϕ ("b" in our notation), thus mimicking a D-residue. The ϕ,ψ values of L-Val at position i+3 (–130°,–50°) belong to the distorted right-handed helical region, with a peculiarly large negative value of ϕ. We classify the α-turn of entry 11 as type PbH2 (model B in Figure 5). Notably, for entry 5, the values of the backbone torsion angles for residues i+1 and i+2 fit nicely with those required for the formation of a type-II β-turn (ideal values: ϕ_{i+1},ψ_{i+1} = –60°,120°; ϕ_{i+2},ψ_{i+2} = 80°,0°). Indeed, entry 5 features a H-bonded C_{10} structure encompassed within the C_{13} structure.

In our notation for the conformational description of α-turns, the mirror image of the type PbH2 discussed above is type pBh2. This latter conformation is adopted by entry 4, of α-turn sequence D-Pro-L-Pro-D-Ala. The ϕ,ψ sets of the three residues are very close in absolute values

but opposite in sign with respect to those of entry 11. Therefore, a type-II′ β-turn takes place at the level of residues i+1 and i+2 within the α-turn.

Entries 3A and 3B are the two independent molecules in the crystals structure of H-L-Tyr-D-Tic-L-Phe-L-Phe-NH_2. For both of them, the D-Tic residue at position i+1 of the α-turn adopts a "p" (type-II polyPro like, ϕ positive) conformation, whereas the two L-Phe residues at positions i+2 and i+3 are located respectively in the right-handed helical and in the bridge (ϕ negative) regions, respectively, of the ϕ,ψ space. Therefore, both entries are classified as type pH1B. Interestingly, a co-crystallized water molecule is H-bonded to molecule 3B, as the donor to the O_i carbonyl oxygen, and as the acceptor to the N_{i+3}-H_{i+3} group, thus giving rise to a water-mediated β-turn.

Finally, the Aib-D-Ala-L-Leu α-turn sequence of entry 7 provides an example of left-handed helical conformation of residue i+1 (the achiral Aib), followed by D-Ala in the bridge (ϕ positive) region, and L-Leu distorted right-handed helical, thus producing a type h1bH2 α-turn.

3.3| Isolated α-turns in cyclic peptides

The occurrence of 51 isolated α-turns in cyclic peptides is documented in 41 crystal structures, ranging from cyclopenta- to cyclododecapeptides (Table 2). Cycles made of eight or more α-amino acid residues provide examples of the occurrence of two isolated α-turns in the same molecule. A significant fraction of the cyclopeptides listed in Table 2 are natural compounds, often characterized by the occurrence in their sequences of N^{α}-methylated and / or side-chain modified α-amino acid residues.

Important, in Table 2 there are 18 entries for which all of the ω torsion angles within the α-turn are found in the usual *trans* disposition (similarly to the α-turn forming linear peptides listed in Table 1), whereas 33 entries are characterized by a *cis* disposition (≅ 0°) of the ω_{i+1} torsion angle. On the basis of this significant conformational difference, ω_{i+1}-*trans* and ω_{i+1}-*cis* α-turns in cyclopeptides will be discussed separately.

3.4| Isolated α-turns in cyclic peptides with ω_{i+1}-*trans*

Similarly to the linear peptides listed in Table 1, for cyclic peptides possessing an all-*trans* disposition of the ω torsion angles within the α-turn (Table 2, entries 1, 2, 17-19, 20a-26b, and 41a-41b), deviations from the value of 180° are in general within ±10°. Larger deviations from exact *trans*-planarity are found for entries 21b (ω_{i+3} = 166°), 22a (ω_{i+3} = 165°), 23 (ω_i = –168°, ω_{i+2} = –163°), 24 (ω_i = –168°, ω_{i+2} = –169°), 26a (ω_{i+2} = 167°), 26b (ω_{i+2} = 158°, ω_{i+3} = –166°), and 41b (ω_i = 167°, ω_{i+3} = –162°).

Among the residues occupying positions i+1, i+2, and i+3 internal to each α-turn, 41 are of L configuration, 6 D, and 7 achiral. Their ϕ,ψ sets are plotted in Figure 6. All of the D residues are characterized by positive values of ϕ except one, located in the lower left quadrant of the ϕ,ψ map. The anomalous position pertains to a D-(αMe)Phe residue (Table 2, entry 1). In this connection, it is worth recalling that a statistical analysis of crystal structures of derivatives and peptides containing this C^{α}-tetrasubstituted, C^{γ}-branched residue highlighted a prevailing "reverse" relationship between (αMe)Phe chirality and helix screw sense (L → left-handed and D → right-handed).[97] The L residues, all of them characterized by negative values of ϕ, are partitioned among the "H1", "H2", "P", and "B" regions of the ϕ,ψ space, in a way not too dissimilar from that of L residues in α-turns of linear peptides shown in Figure 4. The 7 achiral residues are located in region "b" (bridge, ϕ positive).

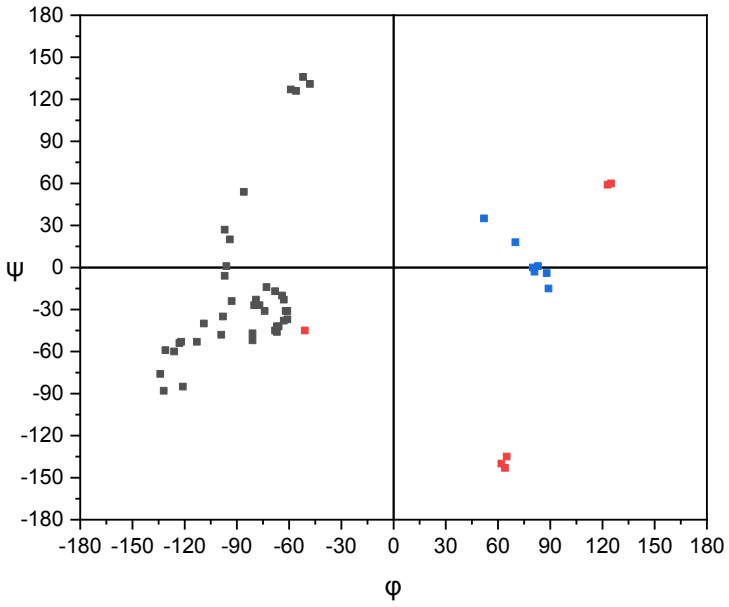

FIGURE 6. Distribution of ϕ,ψ torsion angles for residues at positions i+1, i+2, and i+3 internal to isolated α-turns in the X-ray diffraction structures of cyclic peptides featuring a *trans* disposition for the ω_{i+1} torsion angle. Residues of L configuration in black, D in red, achiral in blue.

Among the 18 entries of Table 2 characterized by a *trans* disposition of the ω_{i+1} torsion angle, there are four examples (entries 18, 19, 21b, 25) in which residues i+1, i+2, and i+3 are all right-handed helical (type H1H1H1 in our α-turn classification). Within this group of entries, the

ϕ,ψ torsion angles (observed ranges: ϕ_{i+1} from –68° to –61°, ψ_{i+1} from –38° to –17°; ϕ_{i+2} from –99° to –66°, ψ_{i+2} from –48° to –42°; ϕ_{i+3} from –81° to –77°; ψ_{i+3} from –52° to –27°) show that on the average the negative ϕ values tend to increase in magnitude on moving from residue i+1 to residue i+3.

Entry 20b provides one example of right-handed helical conformation for both residues i+1 and i+2, but distorted right-handed helical for residue i+3, thus giving rise to a type H1H1H2 α-turn. A β-turn is encompassed within the α-turn. The ϕ,ψ sets of residues i+1 and i+2 (ϕ_{i+1},ψ_{i+1} = –61°,–37°; ϕ_{i+2},ψ_{i+2} = –79°,–23°) allow to classify the β-turn as intermediate between type-I and type-III.

α-Turns for which residue i+1 is located in the "H1" region and residue i+2 in the "B" region of the conformational space are observed for entries 1, 23, and 24. They differ by the conformation adopted by residue i+3, distorted right-handed helical ("H2") for both entries 23 and 24, while left-handed helical ("h1") for entry 1. Therefore, the α-turn of entries 23 and 24 is classified as type H1BH2, whereas that of entry 1 as type H1Bh1. Interestingly, in entries 23 and 24, ϕ_{i+2} is close to –90° and ψ_{i+2} to 0°, and the following i+3 residue of L configuration is distorted right-handed helical. Conversely, for entry 1, the L-Pro residue at position i+2 is found in a conformation still belonging to the "B" region, but characterized by a large and positive ψ value (ϕ_{i+2},ψ_{i+2} = –86°,54°), which allows the following achiral Aib to adopt a left-handed helical conformation. Also, a type-I β-turn is encompassed within the α-turn in entries 23 and 24, but not in entry 1.

For entry 22a, the conformational descriptor of the α-turn is BH1H1. It has to be noted, however, that although the conformation of residue i+1 (ϕ_{i+1},ψ_{i+1} = –73°,–14°) in our classification belongs to the "B" region, the ψ value is very close to the border with region "H1".

Among the α-turns of cyclic peptides featuring a *trans* disposition of the ω_{i+1} torsion angle, we have described nine entries for which residue i+1 is positioned in the "H1" region of the ϕ,ψ map, or in a location of the "B" region close to "H1". The remaining nine entries are characterized by a poly(Pro)$_n$ like conformation of residue i+1, belonging to the "P" region (ϕ negative) or "p" (ϕ positive) depending on its L or D configuration, respectively.

Specifically, for six entries (17, 20a, 21a, 22b, 41a, and 41b), a residue of L configuration at position i+1 is followed by the achiral Gly at position i+2, and by an L residues at position i+3. The sets of ϕ,ψ torsion angles adopted by residues i+1 ($-61° \le \phi_{i+1} \le -48°$, $126° \le \psi_{i+1} \le 136°$), i+2 ($70° \le \phi_{i+2} \le 89°$, $-15° \le \psi_{i+2} \le 18°$) and i+3 ($-134° \le \phi_{i+3} \le -113°$, $-88° \le \psi_{i+3} \le -53°$) allow us to associate the α-turn of all six entries to type PbH2. As remarked in the previous section devoted to linear peptides, this latter conformational descriptor bears the potential for the occurrence of an

intramolecularly H-bonded, type-II β-turn encompassed within the α-turn. This is indeed the case for entries 20a, 21a, 22b, and 41a.

Among the three entries featuring a "p" (ϕ positive) conformation of residue i+1, a D-L-D sequence of the three residues internal to the α-turn characterizes entries 26a and 26b, whereas a D-L-L sequence is adopted in entry 2. Entries 26a and 26b can be assigned to the conformational descriptor pBh2 (mirror image of PbH2). The values of the corresponding torsion angles vary little between the two entries ($62° \leq \phi_{i+1} \leq 65°$, $-140° \leq \psi_{i+1} \leq -135°$; $-97° \leq \phi_{i+2} \leq -94°$, $20° \leq \psi_{i+2} \leq 27°$;$123° \leq \phi_{i+3} \leq 125°$, $59° \leq \psi_{i+3} \leq 60°$). In both entries 26a and 26b, a type-II′ β-turn is encompassed within the α-turn. For entry 2, the ϕ,ψ values of residue i+1 are comparable to those of entries 26a and 26b. However, residues i+2 and i+3 are both right-handed helical, thus allowing us to assign the α-turn of entry 2 to type pH1H1.

3.5| Isolated α-turns in cyclic peptides with ω_{i+1}-*cis*

Among the cyclic peptides listed in Table 2, as many as 33 entries are characterized by a *cis* disposition (≅ 0°) of the ω_{i+1} torsion angle, with values ranging from –17° (entry 7) to 16° (entry 13). Not surprisingly, for all of these cases the peptide bond between residues i+1 and i+2 is a tertiary amide, since position i+2 is occupied by a Pro or an N^{α}-methylated residue. As for the size of cyclopeptides, the ω_{i+1} *cis*-disposition is observed for the only example of hexapeptide (Table 2, entry 3), 13 out of the 14 examples of heptapeptides (entries 4-16), all 8 examples of nonapeptides (entries 27-34), and all 11 examples of α-turn in decapeptides (entries 35a-40), while none for the other cyclopeptide sizes. However, such a correlation between cyclopeptide size and occurrence of the ω_{i+1}-*cis* disposition should be taken with caution. Indeed, within each group of hepta-, nona-, and decapeptides a significant number of entries share sequence similarity (if not identity).

The ϕ,ψ sets of the 99 residues internal to the 33 α-turns characterized by the ω_{i+1}-*cis* disposition are plotted in Figure 7. Only two residues are of D configuration and two are achiral. The only L residue in the lower right quadrant of the Ramachandran map is an L-Ala at position i+3 of entry 3. Most of the other L residues are grouped in the regions "H1" (30 occurrences), "P" (28 occurrences), and "B" (25 occurrences), whereas the "H2" region accounts for 10 occurrences. Interestingly, the ϕ values of the residues belonging to the "H1" region are mainly clustered around –90°, closer to the border with the "H2" region than to the α-helix canonical value (–63°).

To avoid confusion with the conformational descriptors which we exploited for α-turns featuring a *trans* disposition for all of the ω torsion angles, in the case of α-turns characterized by

the ω_{i+1} *cis*-disposition we thought useful to place a "*cis*" in between the symbols used to define the conformation of residues i+1 and i+2.

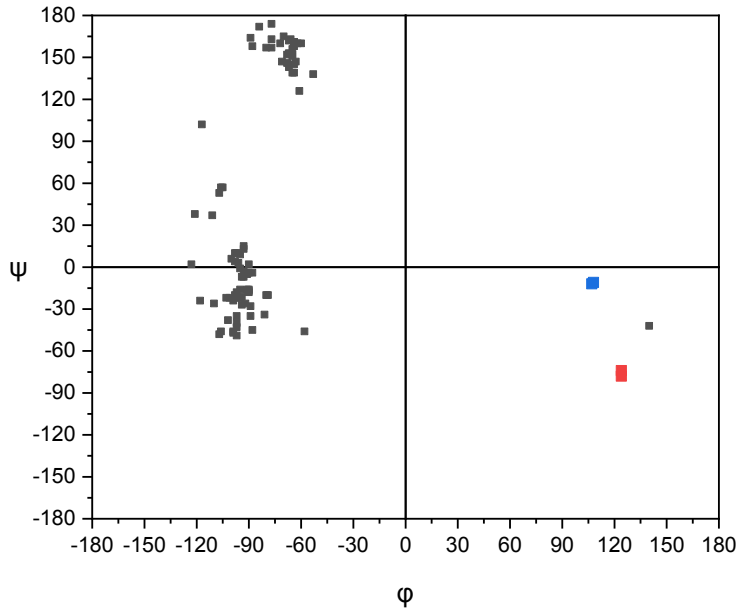

FIGURE 7. Distribution of ϕ,ψ torsion angles for residues at positions i+1, i+2, and i+3 internal to isolated α-turns in the X-ray diffraction structures of cyclic peptides featuring a *cis* disposition for the ω_{i+1} torsion angle. Residues of L configuration in black, D in red, achiral in blue.

Among the 33 entries of Table 2 characterized by a *cis* disposition of the ω_{i+1} torsion angle, there are 18 examples in which residue i+1 is in the "P" (type-II polyPro like, ϕ negative) conformation, residue i+2 belongs to the "B" region, and residue i+3 to "H1". Therefore, the α-turn adopted by entries 7-11, 14-16, 29, 31, 32, 35b, 36a, 36b, 38b, 39a, 39b, and 40 can be defined as type P*cis*BH1 (model C in Figure 5).

Within this group of entries, ϕ_{i+1} values range from –88° to –53° and ψ_{i+1} values from 138° to 165°, whereas ϕ_{i+2} from –111° to –90° and ψ_{i+2} from –7° to 53°. The largest spread of values is observed for ψ_{i+2}, followed by ϕ_{i+1}. The average values for residues i+1 and i+2 (ϕ_{i+1},ψ_{i+1} = –68°,152°; ϕ_{i+2},ψ_{i+2} = –96°,8°) are not far from those typical for an intramolecularly H-bonded β-turn characterized by a *cis* disposition of the central peptide bond, termed type-VI β-turn (ϕ_{i+1},ψ_{i+1} = –60°,120°; ϕ_{i+2},ψ_{i+2} = –90°,0°).[10] Indeed, the occurrence of an intramolecular H-bond between the carbonyl oxygen of residue i and the N-H group of residue i+3, giving rise to a type-VI β-turn encompassed within the α-turn, is observed for entries 7-11 and 14-16. Features common to entries

7-11 and 14-16, to which the onset of the β-turn may be tentatively ascribed, are values of $\psi_{i+1} \leq 151°$ in combination with $\psi_{i+2} \geq 6°$. As for residue i+3, within the "H1" region of the ϕ,ψ space, the ϕ_{i+3} values range from –102° to –58° and ψ_{i+3} from –46° to –16°.

A second group of five entries, namely 5, 6, 33, 37a, and 37b, shares with the group described above conformation "P" for residue i+1 and "B" for residue i+2, but differs in the "H2" conformation adopted by residue i+3. The ϕ,ψ values for residues i+1 and i+2 are well within the ranges observed for type Pc*is*BH1 α-turns, except for the slightly larger ψ_{i+2} value, 57°, for both entries 5 and 6. For these two latter entries, a type-VI β-turn encompassed within the α-turn is observed. In this group of type Pc*is*BH2 α-turns (model D in Figure 5), the ϕ_{i+3} values range from –118° to –106° and ψ_{i+3} from –48° to –24°.

To complete the picture of α-turns characterized by conformations "P" and "B", respectively, for residues i+1 and i+2, concomitantly with a *cis* disposition of the ω_{i+1} torsion angle, entry 4 provides the only example of type Pc*is*BB α-turn. The relevant backbone torsion angles are: $\phi_{i+1},\psi_{i+1} = -61°,126°$; $\phi_{i+2},\psi_{i+2} = -121°,38°$; $\phi_{i+3}, \psi_{i+3} = -123°, 2°$. Also in this case, a type-VI β-turn encompassed within the α-turn is observed.

Another group of six entries (27, 28, 30, 34, 35a, and 38a) can be classified as type Pc*is*H1H1 (model E in Figure 5). The ϕ_{i+1} values range from –67° to –60° and ψ_{i+1} from 158° to 163°. The conformation of residue i+2 is characterized by ϕ_{i+2} values in the range –91° ÷ –79° and ψ_{i+2} from –20° to –16°. These values, although within the "H1" region, are significantly displaced towards the borders with the "B" region, particularly in terms of ψ. As for residue i+3, the ϕ_{i+3} values range from –103° to –97° and ψ_{i+3} from –49° to –22°.

Entries 12 and 13 share the same sequence D-MePhe-L-Pro-Sar for the three residues internal to the α-turn. They provide the only examples, among the entries of Table 2 characterized by a *cis* disposition of the ω_{i+1} torsion angle, of the occurrence of a D residue at position i+1. The values of torsion angles ($\phi_{i+1},\psi_{i+1} = 124°,–74°$ for entry 12, while 124°,–78° for entry 13; $\phi_{i+2},\psi_{i+2} = –77°,174°$ for entry 12, while –84°,172° for entry 13; ($\phi_{i+3},\psi_{i+3} = 107°,–12°$ for entry 12, while 108°,–11° for entry 13) allow us to classify these two α-turns as type p*cis*Pb.

Only one entry of Table 2 remains to be described. Entry 3 features a peculiar sequence of the three residues internal to the α-turn. Specifically, it consists of two side-chain modified L-MeTyr residues followed by L-Ala. The side-chain oxygen atom of L-MeTyr at position i+1 forms an ether bridge with one of the carbon atoms of the aromatic ring of the second L-MeTyr. Such a constraint, beside forcing the ω_{i+1} torsion angle to the *cis* disposition, can be expected to exert a significant influence on the ϕ,ψ torsion angles. Indeed, the ϕ_{i+1},ψ_{i+1} values (–117°,102°) neither

belong to any of the "H1", "H2", "P" or "B" regions characterized by a negative value of ϕ encountered in this survey, nor can be associated to any common peptide / protein conformation. We classify the conformation of residue i+1 as "U" (undefined, ϕ negative). Conversely, residue i+2, with ϕ_{i+2},ψ_{i+2} = –89°,164°, falls in the "P" region, whereas residue i+3 (ϕ_{i+3},ψ_{i+3} = 140° –42°), although of L configuration, belongs to the "b" region (bridge, ϕ positive). As a result, the α-turn observed for entry 3 can be defined as type U*cis*Pb.

4| CONCLUSIONS

The results of our attempt to classify into various types the crystallographically documented isolated α-turns occurring in *peptides* are summarized in Table 3.

For α-turns characterized by the *trans* disposition of all ω torsion angles, twelve types are found. However, by taking into account that two pairs (Ph1h1 / pH1H1, and PbH2 / pBh2) are one mirror image of each other, the significant number of types can be reduced to ten. Among these latter, the most populated type is H1H1H1, accounting to about one third of the occurrences, closely followed by the enantiomeric pair PbH2 / pBh2. The number of occurrences for each of the remaining eight α-turn types varies from three to one.

Conversely, for α-turns characterized by the *cis* disposition of the ω_{i+1} torsion angle, a feature found exclusively in cyclic peptides, only six types are found. Apart from the peculiar type U*cis*Pb (entry 3 of Table 2, see discussion above), the remaining five types share a type-II poly(Pro)$_n$ like conformation (with either ϕ positive or negative) for residue i+1. More than one half of the occurrences populates type P*cis*BH1. Significantly experienced are also type P*cis*H1H1 and P*cis*BH2 (18% and 15% of the occurrences, respectively).

It may be argued that our way of classifying the conformation of each amino acid residue within the α-turn is to some extent questionable, and other alternatives are possible. In particular, the helical ("H1") and distorted helical ("H2") conformations could have been grouped together, or the boundary between "H1" and "H2" in terms of ϕ, as well that between the helical conformations and the bridge ("B") region in terms of ψ, could have been differently placed. Nevertheless our results, taken together, suggest that a significant conformational diversity is compatible with the onset of an intramolecularly H-bonded 13-membered *pseudo*cycle in linear and cyclic peptides.

TABLE 3. Distribution of the occurrence of *isolated* α-turns in peptides among the conformational descriptors exploited in this work. For each α-turn type, ϕ,ψ torsion angles (°) of the three residues internal to the α-turn are reported (average values, except for single occurrences)

α-Turn type	Linear peptides	Cyclic peptides	Total occurrences	ϕ_{i+1}	ψ_{i+1}	ϕ_{i+2}	ψ_{i+2}	ϕ_{i+3}	ψ_{i+3}
H1H1H1	8	4	12	-56	-41	-68	-41	-72	-41
H1H1H2	1	1	2	-60	-32	-77	-24	-109	-33
H1H1B	1		1	-49	-38	-71	-21	-115	-7
H1BH2	1	2	3	-64	-21	-94	-4	-121	-56
H1Bh1		1	1	-51	-45	-86	54	52	35
BH1H1		1	1	-73	-14	-98	-35	-93	-24
Ph1h1	1		1	-59	153	71	39	93	24
pH1H1		1	1	64	-143	-68	-45	-74	-31
PbH2	1	6	7	-57	133	81	0	-126	-66
pBh2	1	2	3	63	-143	-92	26	126	51
pH1B	2		2	64	-153	-73	-33	-119	-8
h1bH2	1		1	59	19	81	1	-112	-36
P*cis*BH1		18	18	-68	152	-96	8	-93	-30
Pc*is*BH2		5	5	-70	152	-99	23	-110	-34
Pc*is*BB		1	1	-61	126	-121	38	-123	2
Pc*is*H1H1		6	6	-64	161	-87	-18	-99	-37
p*cis*Pb		2	2	124	-76	-81	173	108	-12
U*cis*Pb		1	1	-117	102	-89	164	140	-42

REFERENCES

1. Geddes AJ, Parker KD, Atkins EDT, Beighton E. "Cross-β" conformation in proteins. *J Mol Biol.* **1968**; *32*: 343-358.

2. Venkatachalam CM. Stereochemical criteria for polypeptides and proteins. V. Conformation of a system of three linked peptide units. *Biopolymers*. **1968**; *6*: 1425-1436.

3. Lewis PN, Momany FA, Scheraga HA. Chain reversals in proteins. *Biochim Biophys Acta*. **1973**; *303*: 211-229.

4. Toniolo C. Intramolecularly hydrogen-bonded peptide conformation. *CRC Crit Rev Biochem*. **1980**; *9*: 1-44.

5. Smith JA, Pease LG. Reverse turns in peptides and proteins. *CRC Crit Rev Biochem*. **1980**; *8*: 315-399.

6. Richardson JS. The anatomy and taxonomy of protein structure. *Adv Protein Chem*. **1981**; *34*: 167-339.

7. Rose GD, Gierasch LM, Smith JA. Turns in peptides and proteins. *Adv Protein Chem*. **1985**; *37*: 1-109.

8. Crisma M, Formaggio F, Moretto A, Toniolo C. Peptide helices based on α-amino acids. *Pept Sci*. **2006**; *84*: 3-12.

9. Chou PY, Fasman GD. Prediction of β-turns. *Biophys J*. **1979**; *26*: 367-383.

10. Wilmot CM, Thornton JM. Analysis and prediction of the different types of β-turn in proteins. *J Mol Biol*. **1988**; *203*: 221-232.

11. Printz MP, Némethy G, Bleich H. Proposed models for angiotensin II in aqueous solution and conclusions about receptor topography. *Nat New Biol.* **1972**; *237*: 135-140.

12. Némethy G, Printz MP. The γ-turn, a possible folded conformation of the polypeptide chain. Comparison with the β-turn. *Macromolecules.* **1972**; *5*: 755-758.

13. Matthews BW. The γ-turn. Evidence for a new folded conformation in proteins. *Macromolecules*. **1972**; *5*: 818-819.

14. Holmes MA, Matthews BW. Structure of thermolysin refined at 1.6 Å resolution. *J Mol Biol*. **1982**; *160*: 623-639.

15. Flippen JL, Karle IL. Conformation of the cyclic tetrapeptide dihydrochlamydocin. Iabu-L-Phe-D-Pro-LX, and experimental values for 3 → 1 intramolecular hydrogen bonds by X-ray diffraction. *Biopolymers.* **1976**; *15*: 1081-1092.

16. Kawai M, Jasensky RD, Rich DH. Conformational analysis by NMR spectrometry of the highly substituted cyclic tetrapeptides chlamydocin and Ala^4-chlamydocin. Evidence for a unique amide bond sequence in dimethyl sulfoxide-d_6. *J Am Chem Soc*. **1983**; *105*: 4456-4462.

17. Karle IL. Crystal structure and conformation of cyclo-(glycylprolylglycyl-D-alanylprolyl) containing 4 →1 and 3 → 1 intramolecular hydrogen bonds. *J Am Chem Soc.* **1978**; *100*: 1286-1289.

18. Milner-White EJ. Situations of γ-turns in proteins: their relation to α-helices, β-sheets and ligand binding sites. *J Mol Biol.* **1990**; *216*: 385-397.

19. Kalmankar NV, Ramakrishnan C, Balaram P. Sparsely populated residue conformations in protein structures: revisiting "experimental" Ramachandran maps. *Proteins: Struct Funct Bioinf*. **2014**; *82*: 1101-1112.

20. Kishore R, Balaram P. Stabilization of γ-turn conformations in peptides by disulfide bridging. *Biopolymers.* **1985**; *24*: 2041-2043.

21. Crisma M, De Zotti M, Moretto A, Peggion C, Drouillat B, Wright K, Couty F, Toniolo C, Formaggio F. Single and multiple γ-turns: literature survey and recent progress. *New J Chem*. **2015**; *39*: 3208-3216.

22. Pavone V, Gaeta G, Lombardi A, Nastri F, Maglio O, Isernia C, Saviano M. Discovering protein secondary structures. Classification and description of isolated α-turns. *Biopolymers*. **1996**; *38*: 705-721.

23. Nataraj DV, Srinivasan N, Sowdhamini R, Ramakrishnan C. α-Turns in protein structures. *Curr Sci.* **1995**; *69*: 434-447.

24. Ramakrishnan C, Nataraj DV. Energy minimization studies on α-turns. *J Pept Sci*. **1998**; *4*: 239-252.

25. Dasgupta B, Pal L, Basu G, Chakrabarti P. Expanded turn conformations: characterization and sequence-structure correspondence in α-turns with implications in helix folding. *Proteins: Struct Funct Bioinf*. **2004**; *55*: 305-315.

26. Pal L, Chakrabarti P, Basu G. Sequence and structure patterns in proteins from an analysis of the shortest helices: implications for helix nucleation. *J Mol Biol*. **2003**; *326*: 273-291.

27. Cai Y-D, Chou K-C. Artificial neural network model for predicting α-turn types. *Anal Biochem.* **1999**; *268*: 407-409.

28. Chou K-C. Prediction of tight turns and their types in proteins. *Anal Biochem*. **2000**; *286*: 1-16.

29. Chou K-C. Prediction and classification of α-turn types. *Biopolymers*. **1997**; *42*: 837-853.

30. Cai Y-D, Feng K-Y, Li Y-X, Chou K-C. Support vector machine for predicting α-turn types. *Peptides*. **2003**; *24*: 629-630.

31. Narita M, Sode K, Ohuchi S. Single amino acid preferences for specific locations at type-I α-turns in globular proteins. *Bull Chem Soc Jpn*. **1999**; *72*: 1807-1813.

32. Slough DP, McHugh SM, Lin Y-S. Understanding and designing head-to-tail cyclic peptides. *Biopolymers*. **2018**; *109*: e23113.

33. Wang J, Xue Z, Xu J. Better prediction of the location of α-turns in proteins with support vector machine. *Proteins: Struct Funct Bioinf*. **2006**; *65*: 49-54.

34. Kaur H, Raghava GPS. Prediction of α-turns in proteins using PSI-BLAST profiles and secondary structure information. *Proteins: Struct Funct Bioinf*. **2004**; *55*: 83-90.

35. Rose GD. Refraiming the protein folding problem: entropy as organizer. *Biochemistry*. **2021**; *60*: 3753-3761.

36. Rajashankar KR, Ramakumar S. π-Turns in proteins and peptides. Classification, conformation, occurrence, hydration and sequence. *Protein Sci.* **1996**; *5*: 932-946.

37. Dasgupta B, Chakrabarti P. π-Turns. Types, systematics and the context of their occurrence in protein structures. *BMC Struct Biol*. **2008**; *8*: 39.

38. Aravinda S, Shamala N, Balaram P. Aib residues in peptaibiotics and synthetic sequences. Analysis of nonhelical conformations. *Chem Biodivers*. **2008**; *5*: 1238-1262.

39. Schellman C, in Protein Folding, (Ed.: Jaenicke R), Elsevier/North Holland; New York **1980**; 53-61.

40. Groom CR, Bruno IJ, Lightfoot MP, Ward SC. The Cambridge Structural Database. *Acta Crystallogr*. **2016**; *B72*: 171-179.

41. Taylor R, Kennard O, Versichel W. The geometry of the N-H···O=C hydrogen bond. 3. Hydrogen-bond distances and angles. *Acta Crystallogr*. **1984**; *B40*: 280-288.

42. Görbitz CH. Hydrogen-bond distances and angles in the structures of amino acids and peptides. *Acta Crystallogr*. **1989**; *B45*: 390-395.

43. Torshin IY, Weber IT, Harrison RW. Geometric criteria of hydrogen bonds in proteins and identification of "bifurcated" hydrogen bonds. *Protein Eng Des Select*. **2002**; *15*: 359-363.

44. Bruno IJ, Cole JC, Edgington PR, Kessler M, Macrae CF, McCabe P, Pearson J, Taylor R. New software for searching the Cambridge Structural Database and visualizing crystal structures. *Acta Crystallogr*. **2002**; *B58*: 389-397.

45. Macrae CF, Sovago I, Cottrell SJ, Galek PTA, McCabe P, Pidcock E, Platings M, Shields GP, Stevens JS, Towler M, Wood PA. Mercury 4.0: from visualization to analysis, design and prediction. *J Appl Crystallogr*. **2020**; *53*: 226-235.

46. Mir FM, Crisma M, Toniolo C, Lubell WD. Isolated α-turn and incipient γ-helix. *Chem Sci*. **2019**; *10*: 6908-6914.

47. Crisma M, Valle G, Monaco V, Formaggio F, Toniolo C. N^{α}-Benzyloxycarbonyl-α-aminoisobutyrylglycyl-L-isoleucyl-L-leucine methyl ester monohydrate. *Acta Crystallogr*. **1994**; *C50*: 563-565.

48. Flippen-Anderson JL, Deschamps JR, George C, Reddy PA, Lewin AH, Brine GA, Sheldrick G, Nikiforovich G. X-Ray structure of Tyr-D-Tic-Phe-Phe-NH_2 (D-TIPP-NH_2), a highly potent μ-receptor selective opioid agonist. Comparisons with proposed model structures. *J Pept Res*. **1997**; *49*: 384-393.

49. Chatterjee B, Saha I, Raghothama S, Aravinda S, Rai R, Shamala N, Balaram P. Designed peptides with homochiral and heterochiral diproline templates as conformational constraints. *Chem Eur J*. **2008**; *14*: 6192-6204.

50. Scalabrino GA, Hogan N, O'Boyle KM, Slator GR, Gregg DJ, Fitchett CM, Draper SM, Bennett GW, Hinkle PM, Bauer K, Williams CH, Tipton KF, Kelly JA. Discovery of a dual action first-in-class peptide that mimics and enhances CNS-mediated actions of thyrotropin-releasing hormone. *Neuropharmacology*. **2007**; *52*: 1472-1481.

51. Moretto A, De Zotti M, Crisma M, Formaggio F, Toniolo C. N-Methylation of N^{α}-acetylated, fully C^{α}-ethylated, linear peptides. *Int J Pept Protein Res*. **2008**; *14*: 307-314.

52. Rajagopal A, Aravinda S, Raghothama S, Shamala N, Balaram P. Chain length effects on helix-hairpin distribution in short peptides with Aib-DAla and Aib-Aib segments. *Biopolymers (Pept Sci)*. **2011**; *96*: 744-756.

53. Shoenholzer P, Daly JJ, Hennig M. *CSD Commun*. 2000; CCDC 146683. DOI:10.5517/cc4xmqc

54. Hatakeyama Y, Sawada T, Kawano M, Fujita M. Conformational preferences of short peptide fragments. *Angew Chem Int Ed*. **2009**; *48*: 8695-8698.

55. Kar S, Drew MGB, Pramanik A. Formation of vesicles through solvent assisted self-assembly of hydrophobic pentapeptides: encapsulation and pH responsive release of dyes by the vesicles. *Protein Pept Lett*. **2011**; *18*: 886-895.

56. Ballano G, Zanuy D, Jiménez AI, Cativiela C, Nussinov R, Alemán C. Structural analysis of a β-helical protein motif stabilized by targeted replacements with conformationally constrained amino acids. *J Phys Chem B*. **2008**; *112*: 13101-13115.

57. Crisma M, Moretto A, Rainaldi M, Formaggio F, Broxterman QB, Kaptein B, Toniolo C. Crystal-state 3D-structural characterization of novel 3_{10}-helical peptides. *J Pept Sci*. **2003**; *9*: 620-637.

58. Kalita M, Archana A, Dimri A, Vasudev PG, Ramapanicker R. Synthesis of peptides containing oxo amino acids and their crystallographic analysis. *J Pept Sci*. **2019**; *25*: e3148.

59. Arnhold FS, Linden A, Heimgartner H. Synthesis of Aib- and Phe(2Me)-containing cyclopentapeptides. *Helv Chim Acta*. **2015**; *98*: 155-178.

60. Stroup AN, Rockwell AL, Rheingold AL, Gierasch LM. Crystal structure of cyclo(Gly1-L-Pro2-D-Phe3-L-Ala4-L-Pro5): a cyclic pentapeptide with a Gly-L-Pro .delta. turn. *J Am Chem Soc*. **1988**; *110*: 5157-5161.

61. Hitotsuyanagi Y, Sasaki S, Matsumoto Y, Yamaguchi K, Itokawa H, Takeya K. Synthesis of [L-Ala-1]RA-VII, [D-Ala-2]RA-VII, and [D-Ala-4]RA-VII by epimerization of RA-VII, an antitumor bicyclic hexapeptide from *Rubia* plants, through oxazoles. *J Am Chem Soc*. **2003**; *125*: 7284-7290.

62. Iitaka Y, Nakamura H, Takada K, Takita T. An X-ray study of ilamycin B1, a cyclic heptapeptide antibiotic. *Acta Crystallogr*. **1974**; *B30*: 2817-2825.

63. Ma J, Huang H, Xie Y, Liu Z, Zhao J, Zhang C, Jia Y, Zhang Y, Zhang H, Zhang T, Ju J. Biosynthesis of ilamycins featuring unusual building blocks and engineered production of enhanced anti-tubercolosis agents. *Nat Commun*. **2017**; *8*: 391.

64. Sun C, Liu Z, Zhu X, Fan Z, Huang X, Wu Q, Zheng X, Qin X, Zhang T, Zhang H, Ju J, Ma J. Antitubercular ilamycins from marine-derived *Streptomyces atratus* SCS10 ZH16 *ΔilaR*. *J Nat Prod*. **2020**; *83*: 1646-1657.

65. Wu Y, Wu Z-M, Zhang S-S, Liu L-Y, Sun F, Jiao W-H, Wang S-P, Lin H-W. Axinellasins A–D, immunosuppressive cycloheptapeptide diastereomers, discovered via a precursor ion scanning–supercritical fluid chromatography strategy from the marine sponge *Axinella* species. *Org Lett*. **2022**; *24*: 934-938.

66. Rukachaisirikul V, Chantaruk S, Tansakul C, Saithong S, Chaicharernwimonkoon L, Pakawatchai C, Isaka M, Intereya K. A cyclopeptide from the insect pathogenic fungus *Cordyceps* sp. BCC 1788. *J Nat Prod*. **2006**; *69*: 305-307.

67. Chen Z, Song Y, Chen Y, Huang H, Zhang W, Ju J. Cyclic heptapeptides, cordyheptapeptides C–E, from the marine-derived fungus *Acremonium persicinum* SCS10 115 and their cytotoxic activities. *J Nat Prod*. **2012**; *75*: 1215-1219.

68. Vicente J, Vera B, Rodríguez AD, Rodríguez-Escudero I, Raptis RG. Euryjanicin A: a new cycloheptapeptide from the Caribbean marine sponge *Prosuberites laughlini*. *Tetrahedron Lett*. **2009**; *50*: 4571-4574.

69. Pettit GR, Tan R, Herald DL, Williams MD, Cerny RL. Antineoplastic agents. 277. Isolation and structure of phakellistatin 3 and isophakellistatin 3 from a Republic of Comoros marine sponge. *J Org Chem*. **1994**; *59*: 1593-1595.

70. Eggleston DS, Baures PW, Peishoff CE, Kopple KD. Conformations of cyclic heptapeptides: crystal structure and computational studies of evolidine. *J Am Chem Soc*. **1991**; *113*: 4410-4416.

71. Morita H, Kayashita T, Takeya K, Itokawa H, Shiro M. Crystal and solution forms of a cyclic heptapeptide, pseudostellarin D. *Tetrahedron*. **1995**; *51*: 12539-12548.

72. Shoham G, Lipscomb WN, Wieland T. Conformations of amatoxins in the crystalline state. *J Am Chem Soc*. **1989**; *111*: 4791-4809.

73. Kostansek EC, Lipscomb WN, Yocum RR, Thiessen WE. Conformation of the mushroom toxin β-amanitin in the crystalline state. *Biochemistry*. **1978**; *17*: 3790-3795.

74. Shoham G, Rees DC, Lipscomb WN, Zanotti G, Wieland T. Crystal and molecular structure of S-deoxo[Ile3]amaninamide: a synthetic analog of amanita toxins. *J Am Chem Soc*. **1984**; *106*: 4606-4615.

75. Zanotti G, Wieland T, Benedetti E, Di Blasio B, Pavone V, Pedone C. Structure-toxicity relationships in the amatoxin series. Synthesis of S-deoxy[γ(R)-hydroxy-Ile3]-amaninamide, its crystal and molecular structure and inhibitory efficiency. *Int J Pept Prot Res*. **1989**; *34*: 222-228.

76. Kopple KD, Wang Y-S, Cheng AG, Bhandary KK. Conformations of cyclic octapeptides. 5. Crystal structure of cyclo(Cys-Gly-Pro-Phe)$_2$ and rotating frame relaxation (T1.rho.) NMR studies of internal mobility in cyclic octapeptides. *J Am Chem Soc*. **1988**; *110*: 4168-4176.

77. Bhandary KK, Kopple KD. Conformation of cyclic octapeptides. VI. Structure of *cyclo*-bis-(-L-alanyl-glycyl-L-prolyl-L-phenylalanyl-) tetrahydrate. *Acta Crystallogr*. **1991**; *C47*: 1483-1487.

78. Ramalho SD, Wang CK, King GJ, Byriel KA, Huang Y-H, Bolzani VS, Craik DJ. Synthesis, racemic X-ray crystallographic, and permeability studies of bioactive orbitides from *Jatropha* species. *J Nat Prod*. **2018**; *81*: 2436-2445.

79. Silk MR, Price JR, Mohanty B, Leiros H-KS, Lund BA, Thompson PE, Chalmers DK. Side-chain interactions in D/L peptide nanotubes: studies by crystallography, NMR spectroscopy and molecular dynamics. *Chem-Eur J*. **2021**; *27*: 14489-14500.

80. Matsumoto T, Shishido A, Morita H, Itokawa H, Takeya K. Conformational analysis of cyclolinopeptides A and B. *Tetrahedron*. **2002**; *58*: 5135-5140.

81. Di Blasio B, Rossi F, Benedetti E, Pavone V, Pedone C, Temussi PA, Zanotti G, Tancredi T. Bioactive peptides: solid-state and solution conformation of cyclolinopeptide A. *J Am Chem Soc*. **1989**; *111*: 9089-9098.

82. Chitanda JM, Zhu J, Mausberg P, Burnett P-GG, Reaney MJT. [1-9-NαC]-Linusorb B3 (cyclolinopeptide A) acetonitrile disolvate. *IUCrData*. **2016**; *1*: x161706.

83. Di Blasio B, Rossi F, Benedetti E, Pavone V, Saviano M, Pedone C, Zanotti G, Tancredi T. Bioactive peptides: X-ray and NMR conformational study of [Aib5,6-D-Ala8]cyclolinopeptide A. *J Am Chem Soc*. **1992**; *114*: 8277-8283.

84. Schatte G, Labiuk S, Li B, Burnett P-G, Reaney M, Grochulski P, Fodje M, Yang J, Sammynaiken R. Cyclolinopeptide B methanol trisolvate. *Acta Crystallogr*. **2012**; *E68*: o50-o51.

85. Jadhav P, Schatte G, Labiuk S, Burnett P-G, Li B, Okinyo-Owiti D, Reaney M, Grochulski P, Fodje M, Sammynaiken R. Cyclolinopeptide K butanol disolvate monohydrate. *Acta Crystallogr*. **2011**; *E67*: o2360-U514.

86. Chen J-T, Ma R, Sun S-C, Zhu X-F, Xu X-L, Mu Q. Synthesis and biological evaluation of cyclopeptide GG-8-6 and its analogues as anti-hepatocellular carcinoma agents. *Bioorg Med Chem*. **2018**; *26*: 609-622.

87. Saviano M, Rossi F, Filizola M, Di Blasio B, Pedone C. [Aib^{5,6}-D-Ala^{8}]-cyclolinopeptide A, grown from a benzene/acetonitrile mixture. *Acta Crystallogr*. **1995**; *C51*: 663-666.

88. Karle IL, Wieland T, Schermer D, Ottenheim HCJ. Conformation of uncomplexed natural antamanide crystallized from CH_3CN/H_2O. *Proc Natl Acad Sci US*. **1979**; *76*: 1532-1536.

89. Karle IL. [Phe4,Val6]Antamanide crystallized from methyl acetate/*n*-hexane. Conformation and packing. *J Am Chem Soc*. **1977**; *99*: 5152-5157.

90. Karle IL, Duesler E. Arrangement of water molecules in cavities and channels of the lattice of [Phe4,Val6]antamanide dodecahydrate. *Proc Natl Acad Sci US*. **1977**; *74*: 2602-2606.

91. Karle IL. Water structure in [Phe4, Val6] antamanide · $12H_2O$ crystallized from dioxane. *Int J Pept Protein Res*. **1986**; *28*: 6-14.

92. Kessler H, Bats JW, Lautz J, Müller A. Conformation of antamanide. *Liebigs Ann*. **1989**; 913-928.

93. Vasil'ev AD. Structure of crystalline [Phe-1, Ala-9]-antamanide-4-H_2O. *Kristallografiya*. **1993**; *38*: 33-42.

94. Herald DL, Cascarano GL, Pettit GR, Srirangam JK. Crystal conformation of the cyclic decapeptide phakellistatin 8: comparison with antamanide. *J Am Chem Soc*. **1997**; *119*: 6962-6973.

95. Karle IL, Urry DW. Crystal structure of cyclic $(APGVGV)_2$, an analog of elastin, and a suggested mechanism for elongation/contraction of the molecule. *Biopolymers*. **2005**; *77*: 198-204.

96. Pauling L, Corey RB, Branson HR. The structure of proteins. Two hydrogen-bonded helical configurations of the polypeptide chain. *Proc Natl Acad Sci US.* **1951**; *37*: 205-211.

97. Crisma M, Toniolo C. Helical screw sense preferences of peptides based on chiral, C^{α}-tetrasubstituted α-amino acids. *Pept Sci*. **2015**; *104*: 46-64.